Ex Vivo Modeling of Multidomain Peptide Hydrogels with Intact Dental Pulp

A.N. Moore[1], S.C. Perez[1], J.D. Hartgerink[1,2], R.N. D'Souza[3], and J.S. Colombo[3]

Abstract

Preservation of a vital dental pulp is a central goal of restorative dentistry. Currently, there is significant interest in the development of tissue engineering scaffolds that can serve as biocompatible and bioactive pulp-capping materials, driving dentin bridge formation without causing cytotoxic effects. Our earlier in vitro studies described the biocompatibility of multidomain peptide (MDP) hydrogel scaffolds with dental pulp–derived cells but were limited in their ability to model contact with intact 3-dimensional pulp tissues. Here, we utilize an established ex vivo mandible organ culture model to model these complex interactions. MDP hydrogel scaffolds were injected either at the interface of the odontoblasts and the dentin or into the pulp core of mandible slices and subsequently cultured for up to 10 d. Histology reveals minimal disruption of tissue architecture adjacent to MDP scaffolds injected into the pulp core or odontoblast space. Additionally, the odontoblast layer is structurally preserved in apposition to the MDP scaffold, despite being separated from the dentin. Alizarin red staining suggests mineralization at the periphery of MDP scaffolds injected into the odontoblast space. Immunohistochemistry reveals deposition of dentin sialophosphoprotein by odontoblasts into the adjacent MDP hydrogel, indicating continued functionality. In contrast, no mineralization or dentin sialophosphoprotein deposition is evident around MDP scaffolds injected into the pulp core. Collagen III expression is seen in apposition to gels at all experimental time points. Matrix metalloproteinase 2 expression is observed associated with centrally injected MDP scaffolds at early time points, indicating proteolytic digestion of scaffolds. Thus, MDP scaffolds delivered centrally and peripherally within whole dental pulp tissue are shown to be biocompatible, preserving local tissue architecture. Additionally, odontoblast function and pulp vitality are sustained when MDP scaffolds are intercalated between dentin and the odontoblast region, a finding that has significant implications when considering these materials as pulp-capping agents.

Keywords: tissue engineering, regeneration, endodontics, dentin, biocompatibility, extracellular matrix (ECM)

Introduction

Regenerative endodontic therapies aim to create healthy microenvironments that promote the natural healing of dental pulp and timely formation of a tertiary dentin bridge beneath exposed dentinal tubules. Dental caries result from damage to the mineralized tissues of the tooth by attached bacterial biofilms (Farges et al. 2009; Cooper and Smith 2013; Colombo et al. 2014). The dentin-pulp complex has an innate capacity to respond to injury, and this property has provided the basis for the design of various endodontic therapies. Studies aimed at regenerating functional tissues through tissue engineering approaches are increasingly prevalent in the literature, and there has been significant interest in applying these concepts in dentistry (Dobie et al. 2002; Gebhardt et al. 2009; Galler et al. 2012; Cavalcanti et al. 2013; Albuquerque et al. 2014; Colombo et al. 2014).

Pulp capping is a restorative technique employed in an attempt to protect the pulp in the case of full or near exposure by carious lesions. Materials employed in pulp capping include calcium hydroxide–based pastes and mineral trioxide aggregate. These materials have been shown to effectively stimulate tertiary dentin formation, but they can have a deleterious effect on the vitality of pulp tissues, although mineral trioxide

aggregate is much less problematic in this regard than calcium hydroxide (Hirschman et al. 2012; Hilton et al. 2013; Mente et al. 2014; Song et al. 2015). Calcium hydroxide pastes such as Dycal are highly cytotoxic, with 1 study reporting >80% cytotoxicity to the pulp (Furey et al. 2010). Other materials less commonly proposed in the literature include zinc oxide eugenol, glass ionomers, and various adhesive systems (Al-Hezaimi et al. 2011; Mozayeni et al. 2012; Hincapié et al. 2015). Despite efficacy in driving mineralization, these materials are unlikely to be successful in initiating the regeneration of dental pulp, due to their pulpal cytotoxicity, limited biodegradability, and the fact that they bear little structural resemblance to native tissues (Zmener et al. 2012; Kobayashi et al. 2013; Schmalz 2014).

[1]Department of Chemistry, Rice University, Houston, TX, USA
[2]Department of Bioengineering, Rice University Houston, TX, USA
[3]School of Dentistry, University of Utah, Salt Lake City, UT, USA

A supplemental appendix to this article is published electronically only at http://jdr.sagepub.com/supplemental.

Corresponding Author:
J.S. Colombo, Room 295B, Biopolymers Research Building, University of Utah, Salt Lake City, UT 84112, USA.
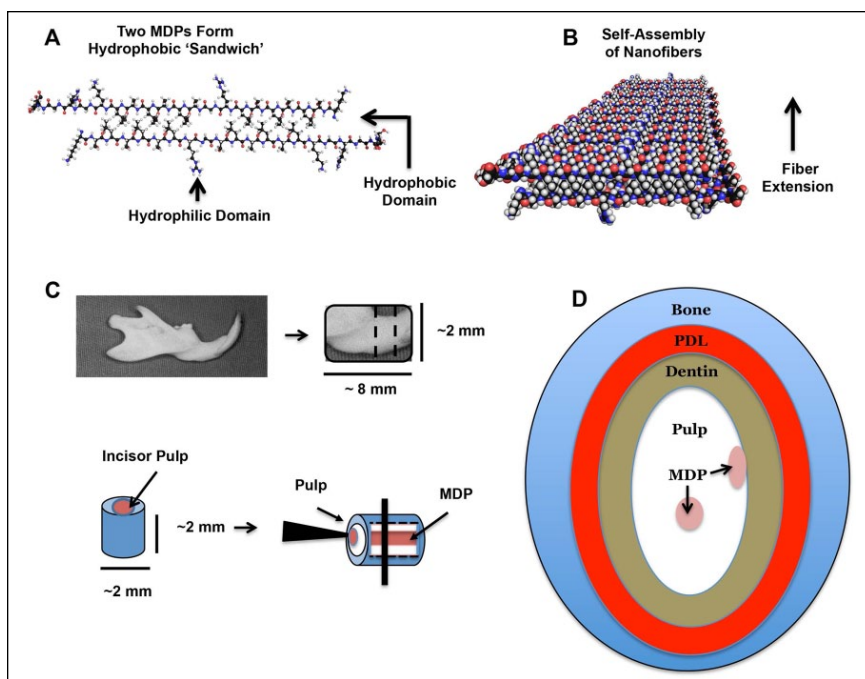Email: John.Colombo@hsc.utah.edu

Figure 1. Multidomain peptide (MDP) scaffold self-assembly and injection. (**A**–**B**) Self-assembly of MDP scaffolds. (A) Two individual MDP subunits align to form a hydrophobic "sandwich" to minimize contact of hydrophobic side chains with the surrounding aqueous environment. (B) Multiple hydrophobic sandwiches assemble to form nanofibers, driven by the formation of hydrogen bonds between adjacent peptide backbones. (**C**–**D**) Preparation of ex vivo mandible slice organ culture model and injection of MDP scaffold. (C) Mandibles were dissected out, cleaned of attached soft tissues, and sliced into 2-mm sections on a phosphate buffered saline–cooled rotary bone saw. MDP scaffolds were injected into both the pulp core and the odontoblast space in columns running the entire length of the incisor pulp. (D) Schematic of an injected mandible section showing the relative position of the tissues and MDP. Injected mandible sections were cultured for 1, 4, 7, and 10 d.

There is a pressing need to develop biocompatible and bioactive materials to provide more effective, biologically based therapies. Multidomain peptide (MDP) scaffolds have demonstrated promise as injectable, bioactive, and biodegradable hydrogel scaffolds for tissue regeneration (Galler et al. 2010; Galler et al. 2012; Kumar, Taylor, Shi, Wang, et al. 2015; Kumar, Taylor, Shi, Wickremasinghe, et al. 2015). In terms of structure, MDPs consist of short sequences of amino acids that self-assemble to form fibers in aqueous solution (Fig. 1A, B). Through noncovalent cross-linking of these fibers, a hydrogel is formed bearing structural resemblance to the native extracellular matrix. Alteration of peptide primary sequence allows for easy customization of the hydrogel scaffold, and loading of the hydrogel with various bioactive factors has provided successful delivery of these factors in previous studies (Galler et al. 2012). These materials have also been shown to have an inherent level of bacterial toxicity while remaining harmless to mammalian cells (Xu et al. 2014). Aiding clinical applicability of these scaffolds, MDP hydrogels shear recover, providing an injectable scaffolding material that can easily be delivered to the tissue of interest while invoking minimal damage on the surrounding tissue. Sequence $K(SL)_3RG(SL)_3KGRGDS$ has demonstrated biocompatibility with NIH-3T3 fibroblasts, DPSCs, and stem cells from human exfoliated deciduous teeth (SHED) cells (Galler et al. 2012). The primary sequence of this peptide hydrogel offers susceptibility to matrix metalloproteinase 2 (MMP-2) enzymatic degradation and promotes cell attachment via integrin binding; the incorporation of these bioactive motifs has resulted in increased viability, migration, and spreading in in vitro studies of SHED cells (Galler et al. 2010; Kang et al. 2014). In an in vivo study involving immunocompromised mice, this MDP hydrogel loaded with vascular endothelial growth factor (VEGF), transforming growth factor beta 1 (TGFβ1), and FGF2 has regenerated pulplike connective tissue within dentin cylinders implanted subcutaneously in the mouse (Galler et al. 2012). Thus, we propose that these scaffolds provide a highly tunable, easily loaded biocompatible scaffold with optimal physical properties for introduction to pulp tissues, particularly in pulp-capping procedures. Through the use of a biomimetic material, we aim to preserve and enhance native biological responses within pulp tissue.

Ideally, to determine the efficacy of a tissue engineering material in driving the regeneration of a given tissue, the material should be placed in contact with the tissue that it seeks to regenerate. Thus, central to the development of regenerative dental materials is the development of model systems that reflect the complexity of the specialized tissues of the oral cavity. Smith and colleagues (2010) extensively characterized a rat mandible slice organ culture model that gives access to the mandibular bone, periodontal ligament, and, critically, dental pulp tissue. Slices can be cultured for up to 21 d, maintaining viability, normal tissue architecture (including a distinct odontoblast layer), and active synthesis and deposition of collagen by odontoblasts. It has also been used as an organ culture system to examine the migration and behavior of labeled mesenchymal progenitor cells (Colombo et al. 2015). A similar model system has been employed to investigate osteoclast development during periodontal inflammation using mouse mandibles (Sloan et al. 2013). These models give a unique ability to examine and characterize the interactions of novel bioactive pulp-capping materials with complex pulp tissue. While this model does not replace preclinical models, as it notably lacks a blood supply, it is ideal for investigating odontoblast and pulpal fibroblast cell interactions with tissue engineering scaffolds within their native extracellular matrix environment.

Here, we aim to use a complex ex vivo mandible slice organ culture system to evaluate MDP scaffolds in the localized pulp of the odontoblast space and core. We hypothesize that MDP hydrogels demonstrate cellular compatibility in pulp tissue,

preserving tissue-specific and biologically appropriate activity in these tissues.

Materials and Methods

Peptide Synthesis and Scaffold Preparation

K(SL)$_3$RG(SL)$_3$KGRGDS was synthesized at a 0.45-mmol scale via an automated Focus XC Solid Phase Peptide Synthesizer (AAPPTec, Louisville, KY, USA), with methods previously described (Aulisa et al. 2009). The N- and C-termini of the peptide were acetylated and amidated, respectively, and the peptide was dialyzed with benzoylated dialysis tubing (MWCO: 2000, Sigma-Aldrich, St. Louis, MO, USA) following cleavage of the peptide from the resin. Correct molecular mass was confirmed through MALDI-TOF mass spectrometry. The peptide was lyophilized and subsequently dissolved in MilliQ water at a concentration of 20 mg/mL. Hydrogels were prepared by adding equal volumes of peptide solution (20 mg/mL) and HBSS (1×, Mediatech, Inc., Manassas, VA, USA) containing 300 mM of sucrose; thus, the final concentration of peptide was 10 mg/mL, and the final concentration of sucrose was 150 mM in the hydrogel.

Mandible Harvest, MDP Delivery, and Organ Culture

Wistar rats (Charles River Laboratories, Wilmington, MA, USA) approximately 28 d old were obtained and their mandibles harvested following Rice University's Institutional Animal Care and Use Committee (protocol A13042501). Using a low-speed saw (IsoMet; Buehler, Düsseldorf, Germany), the ramus, condyle, and incisor were removed from the mandible, and the remaining portion was cut into 2-mm-thick sections. A 33-gauge needle (World Precision Instruments, Sarasota, FL, USA) was used to inject approximately 5 μL of MDP hydrogel scaffold into either the pulp core or the odontoblast space (Fig. 1C, D). This volume was determined as the amount required to backfill a column through the pulp of each mandible slice given the diameter of the injection needle. Elapsed time from mandible harvest to completion of injection was <45 min for all samples, and samples were kept in α-MEM media (Gibco, Grand Island, NY, USA) containing 10% fetal bovine serum (Life Technologies, Grand Island, NY, USA), 10% penicillin/streptomycin (Gibco), and 1% L-ascorbic acid 2-phosphate (Sigma-Aldrich) during preparation. Samples were cultured in α-MEM media containing 10% fetal bovine serum, 1% penicillin/streptomycin, and 1% L-ascorbic acid 2-phosphate at 37 °C and 5% CO$_2$ with media exchange performed every 48 h. For all experiments, there were 5 injected mandible slices for each time point.

Histology

Mandible sections were cultured for 1, 4, 7, or 10 d. These time points were selected due to reported decreases in pulp core cell numbers after 14 d (Smith et al. 2010) and to correspond with previous in vitro studies using this scaffold system (Kang et al. 2014). Subsequently, samples were fixed in 10% buffered formalin (Fisher Scientific, Pittsburgh, PA, USA) overnight and partially demineralized in 10% formic acid (VWR, Radnor, PA, USA) for 48 to 72 h to allow for sectioning of the tissue. To preserve the hydrogel during cryosectioning, samples were soaked in HistoPrep (Fisherbrand, Fair Lawn, NJ, USA) overnight at 4 °C (Ruan et al. 2013). The following day, samples were rinsed and embedded in OCT Compound (Tissue-Tek, Torrance, CA, USA) and flash-frozen in dry ice/ethanol slurry. Ten-micrometer-thick tissue sections were obtained via cryosectioning and adhered to SuperFrost Plus Microscope Slides (VWR). Hematoxylin and eosin and Masson's trichrome staining were performed to visualize tissue architecture and collagen deposition. Alizarin red S (2% w/v in MilliQ water, pH 4.2; Sigma-Aldrich) was applied for 3 min to stain calcium (Colombo et al. 2011; Ng et al. 2014). After staining, slides were mounted with DPX mountant (Sigma-Aldrich) and imaged with an Evos XL Core microscope (Electron Microscopy Sciences, Hatfield, PA, USA).

Immunohistochemistry

Antigen retrieval was performed by immersing tissue sections in sodium citrate buffer (10mM sodium citrate, 0.05% Tween-20, pH 6.0) at 100 °C for 30 min. Subsequently, tissue sections were permeabilized in 0.5% Triton-X and blocked in 1% bovine serum albumin for 30 min. Immunostaining for dentin sialophosphoprotein (DSPP) was performed with a 1:125 dilution of anti-rat DSPP antibody (Millipore, Billerica, MA, USA; D'Souza et al. 1992). Collagen III was detected with an anti-rat type III collagen antibody in a 1:250 dilution (Sigma-Aldrich). MMP-2 expression was visualized with anti-rat MMP-2 antibody at a 1:50 dilution (Bioss, Woburn, MA, USA). For DSPP and type III collagen immunostains, Alexa Fluor 555 Donkey Anti-Mouse IgG antibody was used as the secondary antibody, while Alexa Fluor 568 Donkey Anti-Rabbit IgG antibody was used as the secondary antibody for MMP-2 detection (Invitrogen, Grand Island, NY, USA). Secondary antibodies were used at a 1:500 dilution. Sections were mounted with ProLong Gold with DAPI solution prior to imaging with a Nikon A1-Rsi confocal system (Life Technologies). Instrument gain and settings were set for each immunostaining reaction and kept constant while sections from all time points were imaged.

Results

Histology

Delivery of MDP scaffold to both the odontoblast space and the pulp core was achieved with minimal disruption of surrounding pulp tissue (Fig. 2A–C). At day 1 post-injection, the odontoblast layer appears to be retracted from the dentin but still intact, as columnar odontoblast cells are clearly visible in apposition to the injected scaffold (Fig. 2D). From day 4 to day
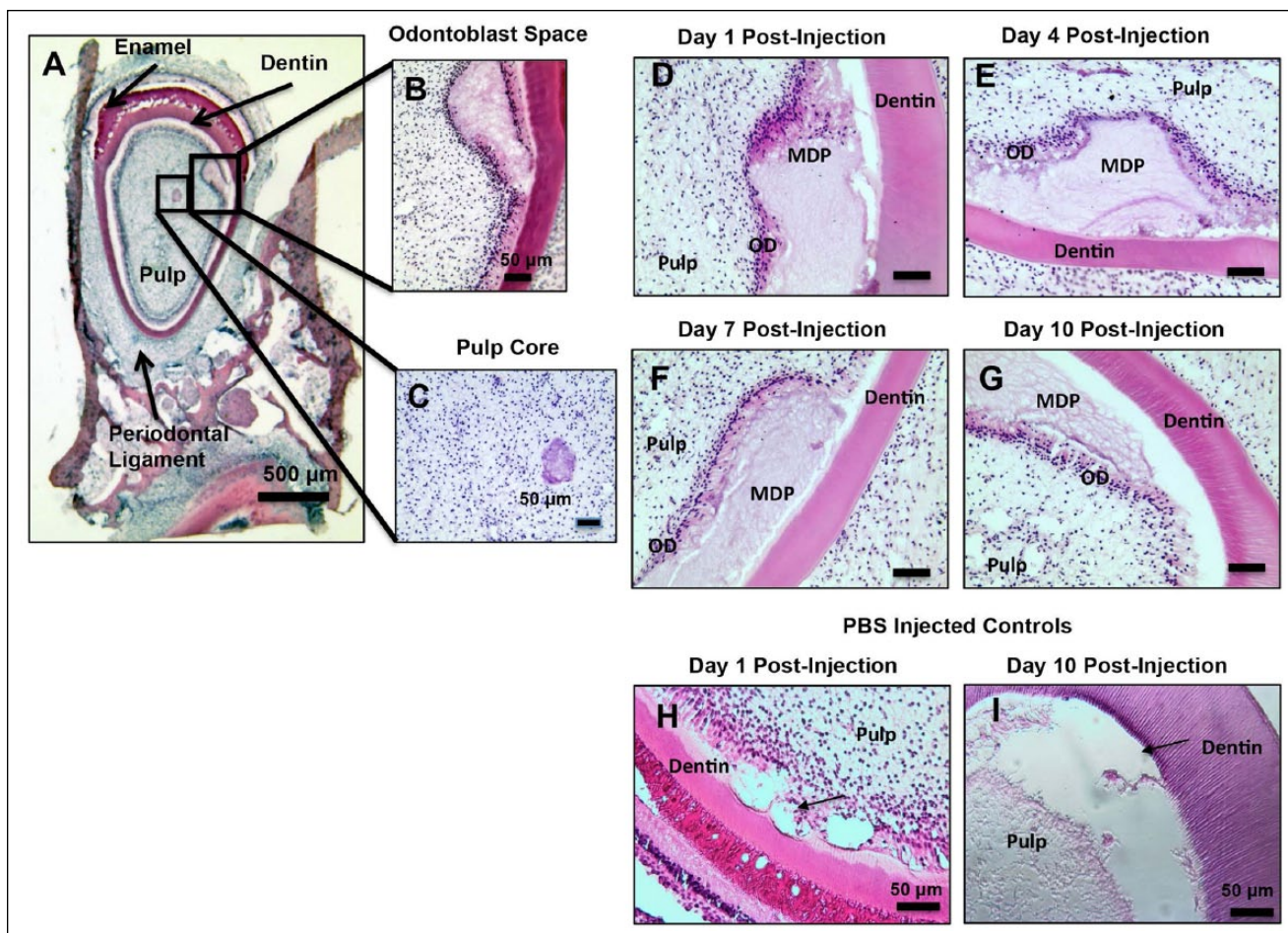
Figure 2. Hematoxylin and eosin (H&E) histology of odontoblast (OD) layer injected multidomain peptide (MDP). (**A–C**) Histology showing MDP scaffolds injected into the OD space and the pulp core. (**D–G**) H&E–stained sections at all post-injection time points, showing a surviving OD layer in apposition to the injected MDP scaffolds. (**H, I**) Phosphate buffered saline (PBS)–injected controls after 1 and 10 d in culture. Arrows indicate injection sites. The OD layer is partially ablated by PBS injection at day 1 post-injection. Pulp vitality of PBS-injected controls declines substantially at 10 d post-injection, and there is a loss of a discreet OD layer. Scale bars = 100 μm where not otherwise indicated.

10, a reestablished layer of odontoblasts with columnar cell bodies is seen in close contact with the MDP scaffold (Fig. 2E–G). The MDP scaffold appears morphologically different over time, with scaffolds at early time points appearing more solid with small fibrillar structures visible. At later time points, these fibrillar structures become much more prominent, with large fibrillar structures visible throughout injected scaffolds by day 10 post-injection (Fig. 2G). Throughout the culture period, the tissue architecture of the dental pulp, periodontal ligament, and bone is maintained. In phosphate-buffered saline (PBS)–injected controls, the pulp detaches from the dentin over the culture period and appears nonvital, with few visible nuclei (Fig. 2H–I). Masson's trichrome staining demonstrated blue staining in the odontoblast cell layer, but there was not consistent blue staining within injected MDP scaffolds to indicate collagen deposition over the culture period (Fig. 3A–D). The odontoblast region was otherwise undisturbed, as evidenced by normal histology at uninjected areas of the odontoblast region at all post-injection time points (Appendix Fig.

1A, B). This is consistent with uninjected mandible slices (Appendix Fig. 1C) and with previously published results of uninjected mandible slices (Smith et al. 2010; Sloan et al. 2013; Roberts et al. 2013; Colombo et al. 2015).

Alizarin Red Staining

Light red staining indicating the continued presence of calcium was observed in the adjacent odontoblast layer as early as day 1 post-injection (Fig. 3E). By day 4 post-injection, bright red staining appears in both the odontoblast layer and the adjacent injected MDP (Fig. 3F), forming a zone of increased calcium within the gel most closely associated with the odontoblast layer. Figure 3G and H demonstrate the continued presence of this high-calcium zone within the injected MDP in apposition to the odontoblast layer at days 7 and 10 post-injection. Uninjected areas of the odontoblast region showed typical light red staining, as did dentin and bone tissues. Pulp tissue and periodontal ligament remained unstained (Appendix Fig. 1D).
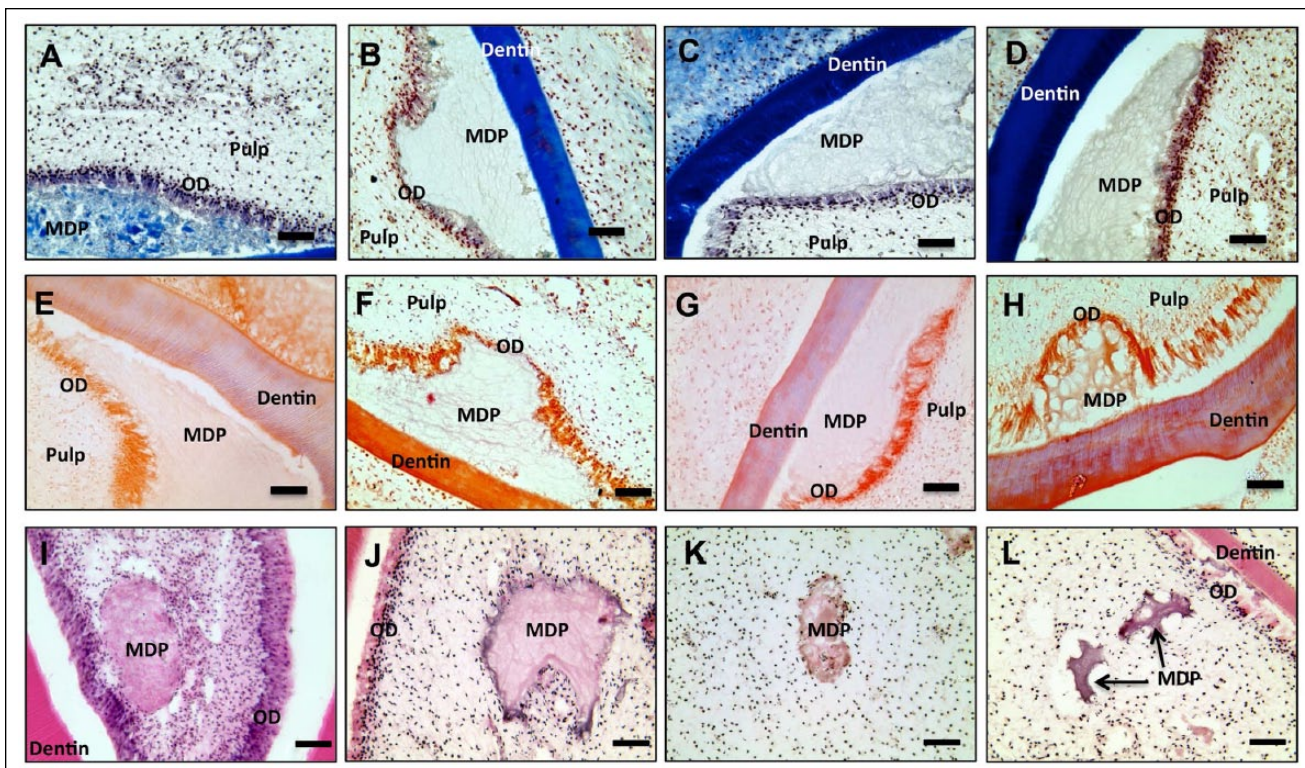
Figure 3. Masson's and alizarin red staining of odontoblast (OD) layer injected multidomain peptide (MDP). Hematoxylin and eosin (H&E) histology of pulp core–injected MDP. Masson's trichrome–stained sections at day 1 (**A**), day 4 (**B**), day 7 (**C**), and day 10 (**D**) showing a surviving OD layer stained light blue, suggesting continued collagen production. Alizarin red–stained sections at day 1 (**E**), day 4 (**F**), day 7 (**G**), and day 10 (**H**). Bright red staining at the OD–MDP scaffold interface indicates elevated local calcium levels, particularly at 4, 7, and 10 d post-injection. H&E histology showing the degradation of pulp core–injected MDP scaffolds over time. At day 1 post-injection (**I**), the delivered MDP scaffold has rounded edges. At days 4 (**J**) and 7 (**K**) post-injection, evidence of cell incursion at the scaffold periphery is visible, although deep penetration of pulp cells into the scaffold was not observed. At day 10 post-injection (**L**) fragments of MDP scaffold are visible, and degradation appears to have advanced. Complete remodeling has not been achieved by day 10 post-injection. Scale bars = 50 μm.

DSPP Expression

DSPP immunohistochemistry reveals expression of DSPP in both the odontoblast cell layer and the adjacent MDP scaffold at all time points (Fig. 4). The intensity of staining increases with culture time, with relatively high levels of expression observed at days 7 and 10 post-injection (Fig. 4C, D). The distribution of DSPP expression corresponds with the large fibrillar structures in the MDP scaffold apparent in the histology at days 7 and 10 post-injection. Dentin tubules stain positive for DSPP at all time points and serve as a positive control (Appendix Fig. 1E). Due to the relative brightness of the signal from the gel, it was difficult to show odontoblast layer expression of DSPP using fluorescence, as the signal was relatively weaker in this region. Therefore, odontoblast layer expression of DSPP was confirmed by diaminobenzidine peroxidase staining with the same anti-DSPP primary antibody and is consistent at both injected and uninjected sites (Appendix Fig. 2A, B). DSPP expression is not evident at any post-injection time point in MDP scaffolds injected into the pulp core, which are not in contact with the odontoblast layer (Fig. 4F). Primary excluded negative controls show no staining in the odontoblast space, pulp core–injected MDP hydrogels, or dentin tubules (Fig. 4E, Appendix Fig. 3).

Collagen III and MMP-2 Expression

The distribution of collagen III associated with pulp core–injected MDP was roughly the same at all time points (Fig. 5). While present in the pulp core at days 1 and 4 post-injection (Fig. 5A, B), collagen III staining intensity noticeably increases at days 7 and 10 post-injection (Fig. 5C, D), particularly at the interface with the injected MDP, suggesting higher levels of expression in these areas. Primary excluded controls show no signal (Fig. 5G, Appendix Fig. 4). The pulp tissue remained positive for collagen III over the culture period, suggesting maintenance of normal pulp matrix in the presence of MDP scaffolds.

Immunohistochemistry for MMP-2 reveals expression by cells around the margins of MDP scaffolds injected into the pulp core at days 1 and 4 post-injection (Fig. 5E, F). This corresponds with histologic evidence of hydrogel degradation around the margins of the scaffold over time (Fig. 3I–L). At days 7 and 10, MMP-2 expression around injected scaffolds is substantially reduced. MMP-2 expression is not present around MDP scaffolds injected into the odontoblast space at any time point. Primary excluded controls show no signal (Fig. 5H, Appendix Fig. 5).
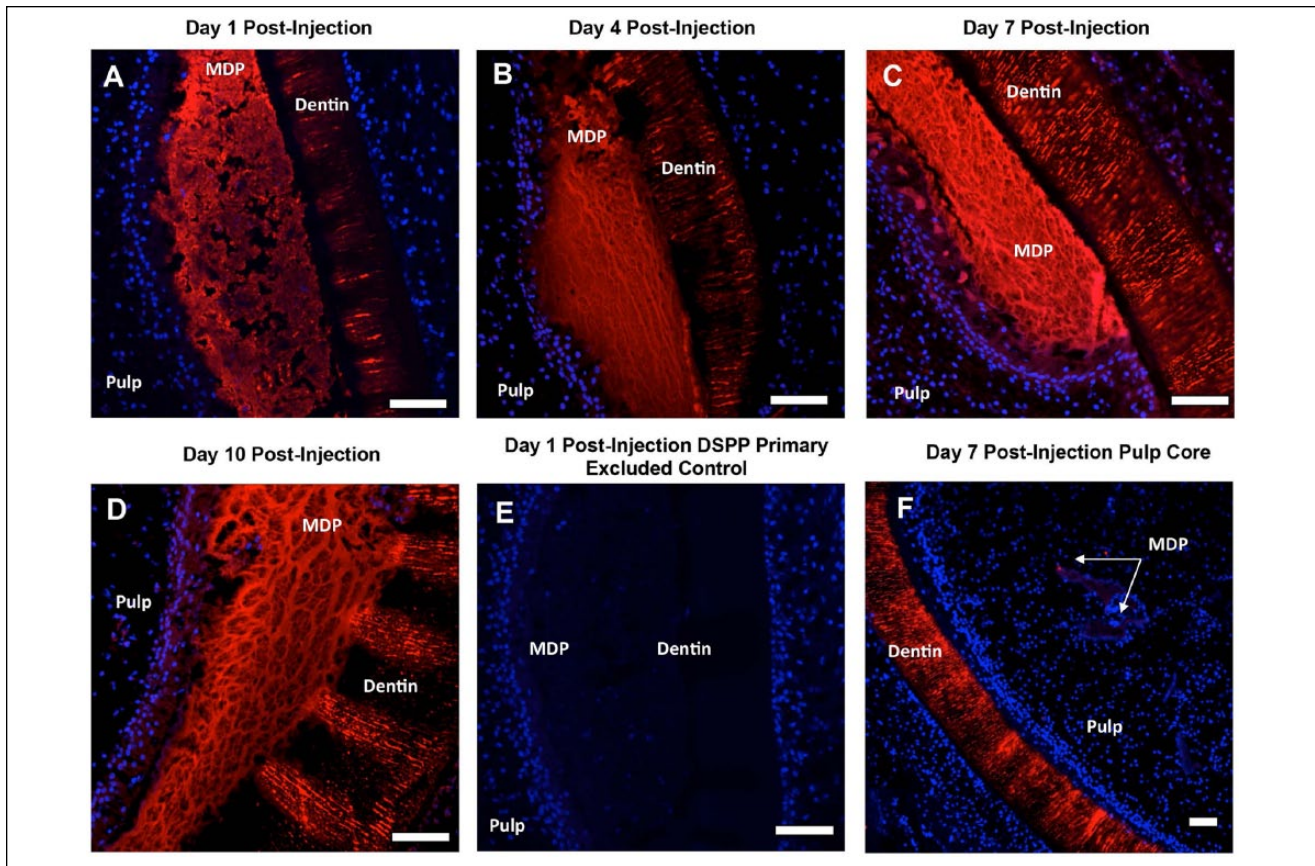
Figure 4. Dentin sialophosphoprotein (DSPP) immunostaining of multidomain peptide (MDP) injected into the odontoblast space of mandible slices at days 1, 4, 7, and 10 post-injection. (**A–D**) Positive staining is observed in the injected MDP scaffold at all post-injection time points. DSPP positive staining is also observed in the adjacent odontoblast layer. This is most prominent at days 7 and 10 post-injection. (**E**) A representative DSPP primary antibody excluded control at 1 d post-injection showing no positive staining. Primary excluded controls were negative at all post-injection time points. (**F**) A representative image of DSPP immunostaining of MDP injected into the pulp core at 7 d post-injection. DSPP is not detected in the pulp core or associated with MDP scaffolds injected into the pulp core at any post-injection time point. Red, positive staining; blue, DAPI-stained nuclei. Scale bars = 100 µm.

Discussion

We previously demonstrated cytocompatibility between dental pulp–derived mesenchymal cells and MDP scaffolds in vitro (Galler et al. 2010; Kang et al. 2014). Results from these studies have been valuable in assessing the biocompatibility, biomechanical properties, shear recovery capacity, and biodegradable nature of these scaffolds. However, such in vitro approaches are limited and cannot provide a method of studying interactions between MDP scaffolds and intact tissues. Ex vivo mandible organ culture allows for robust modeling of the detailed interactions between biomaterials and dental tissues, as it permits the placement of biomaterials into a 3-dimensional pulp environment. We have demonstrated that MDP hydrogels can be injected into the incisor pulp without destruction of the native tissue and that local responses to a biomaterial can be examined for up to 10 d of culture.

Since primary odontoblasts are difficult to isolate and culture under physiologic conditions, it is challenging to accurately assess their response to dental materials or examine their behavior under an altered local environment. Therefore, the injection of MDP in

columns through the mandible slices maximizes the contact between intact odontoblasts and the scaffold while observing the reaction of a heterogeneous population of pulpal cells.

An interesting finding of our studies is the observation of an intact layer of odontoblasts in apposition to the MDP scaffold at all time points (Fig. 2). It appears that, despite the distention of the odontoblast layer caused by the injection of the scaffold, odontoblast viability is restored and sustained. The deleterious effects of PBS injection into the odontoblast layer do not result from a directly cytotoxic effect of PBS but possibly from the mechanical detachment of odontoblasts from the dentin, thereby compromising the structural integrity of the tissue. In contrast, PBS injection into the pulp core does not have a deleterious effect on pulp vitality (Colombo et al. 2015). It may be that the continued vitality of dental pulp is dependent on mechanical support provided by the odontoblasts in association with dentin, here provided by the injected MDP scaffold. Similarly, preliminary experiments involving the insertion of Dycal into the odontoblast space resulted in cell death within the odontoblast layer and pulp core (Appendix Fig. 1F). As a substantial disruption of the odontoblast layer is not observed
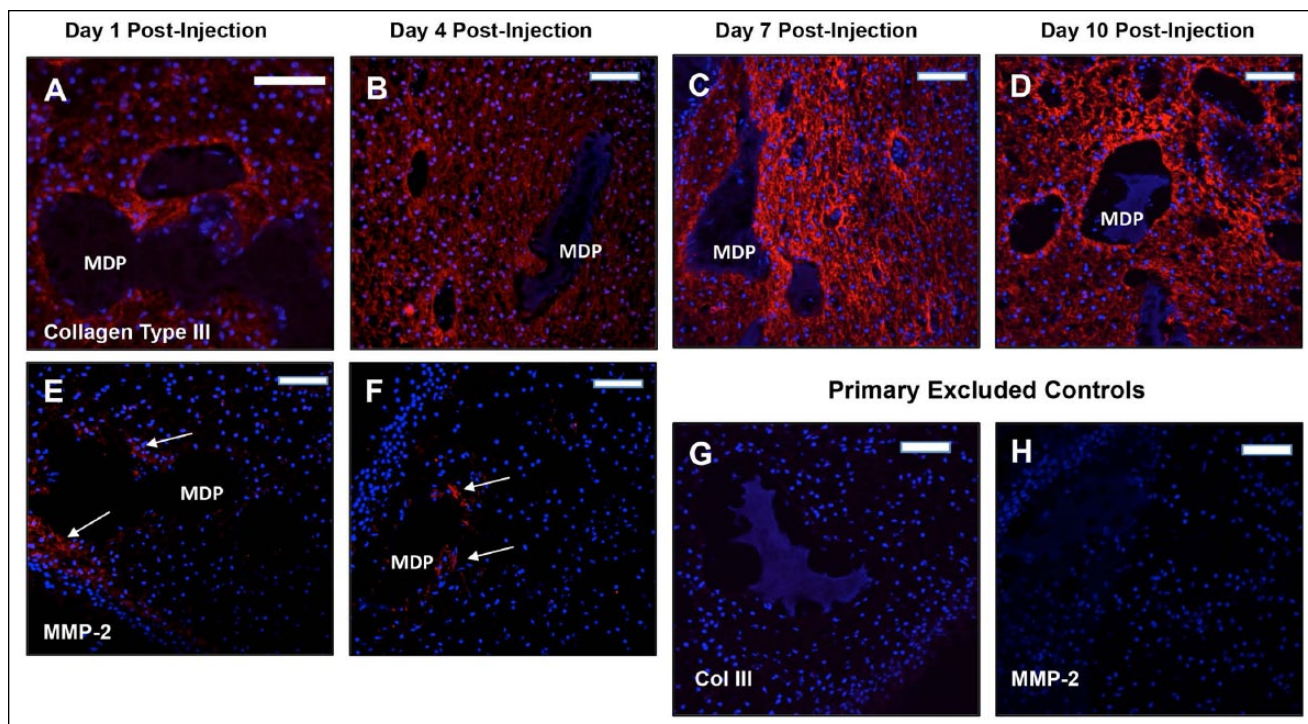
Figure 5. Collagen type III and matrix metalloproteinase 2 (MMP-2) immunostaining associated with pulp core–injected multidomain peptide (MDP) scaffolds. (**A–D**) Collagen III positive staining is seen throughout the pulp tissue at all post-injection time points as expected. Staining intensity increases in apposition to the injected MDP scaffolds at days 7 and 10 post-injection. (**E, F**) MMP-2 positive staining is associated with pulp core–injected MDP scaffolds at days 1 and 4 post-injection. MMP-2 expression was not observed at days 7 and 10 post-injection. Positive staining is indicated by arrows. (**G, H**) Representative primary antibody–excluded controls for collagen type III at day 10 post-injection and MMP-2 at day 4 post-injection. Controls were negative at all post-injection time points. Collagen type III and MMP-2 positive staining were not observed in the odontoblast layer adjacent to odontoblast space–injected MDP scaffolds. Red, positive staining; blue, DAPI-stained nuclei. Scale bars = 100 μm.

at days 1 or 4 post-injection, it is probable that the odontoblasts seen in apposition to MDP scaffold at days 7 and 10 are not newly recruited but rather represent the original population lining the dentin-pulp interface.

Expression of DSPP within MDP scaffolds injected into the odontoblast space (Fig. 4), along with evidence of mineralization at the edges of injected MDP scaffolds (Fig. 3E–H), suggests that the odontoblasts in apposition to scaffolds are synthetically active and are attempting to remodel the scaffold into dentin matrix. While DSPP could be leaching from the dentin into the scaffold, continued expression of DSPP in the odontoblast cell layer shows that these cells remain synthetically active at all post-injection time points. Furthermore, the lack of DSPP expression within hydrogels injected into the pulp core implies that DSPP immunostaining in MDPs injected beneath odontoblasts is not an artifact or the result of nonspecific staining. The structure of the MDP hydrogel selected for use in these studies resembles that of type I collagen, suggesting that the hydrogel provides a suitable substrate for the deposition and sequestration of noncollagenous proteins such as DSPP, as is known to occur during primary dentin formation.

Cells within the pulp core appear to respond differently to the MDP hydrogel when compared with the more peripherally located odontoblast population, indicated by a lack of DSPP signal within hydrogels delivered to the pulp core rather than the odontoblast space (Fig. 4F). While a mineralizing response

by odontoblasts is desirable in the marginal pulp, ectopic tertiary dentin production in the pulp core could result in pathologic conditions such as pulp stones. In contrast, the MDP hydrogel appears biocompatible with native pulp tissue, with no deleterious effects to surrounding tissue architecture observed. Expression of extracellular matrix proteins at the interface between hydrogel and native pulp seems to increase over time, suggesting hydrogel remodeling and pulp soft tissue matrix deposition at this interface. The expression of MMP-2 around the pulp core–injected MDP scaffolds supports this, indicating cellular-mediated degradation of the hydrogel at earlier post-injection time points.

In contrast to materials such as Dycal, MDP scaffolds appear to preserve the normal mineralizing activity of odontoblasts without inflicting tissue damage or notable cytotoxicity. Previous in vitro and in vivo studies showed that MDP hydrogels are capable of absorbing and delivering the secretome of embryonic stem cells (Bakota et al. 2011), and the MDP appears to play a similar role in the pulp tissue. Injected scaffolds appear to act as a reservoir for DSPP, retaining it after active secretion by existing odontoblasts within this culture system. The clinical implications for these findings are significant when considering MDP as a material that could be applied underneath a restoration to encourage dentin bridge formation by interacting with resident odontoblasts, without damaging pulp tissue in contact with the scaffold.

To effectively restore tissue structure and function, biomaterials must promote healing and regeneration while having minimal deleterious effects. Ideally, the material should also be degraded during tissue remodeling. Using a model that allows detailed characterization of intact pulp tissue, we now demonstrate that injectable MDP hydrogel scaffolds exhibit biocompatibility and the capacity to undergo differential remodeling at separate anatomic locations within the pulp. The preserved native response of the odontoblast layer to directly applied MDP scaffolds in particular has interesting implications for clinical use in restorative dentistry. Due to the physical properties and biocompatibility of MDP scaffolds, they can easily integrate bioactive factors and enriched populations of mesenchymal progenitor cells for delivery into pulp tissues, a potentially significant advantage over current pulp-capping materials. Furthermore, the ex vivo organ culture system developed here can be used to assess whether the delivery of bioactive factors from these matrices optimizes a tissue regenerative response.

While this study elucidates the local effects and tissue response to this biomimetic scaffold, it stops short of examining the systemic responses mediated by the cardiovascular and immune systems. MDP scaffolds injected into the dorsal space of rats have been shown to be highly permeable to cells from the blood supply, highlighting the importance of the vasculature to the healing response (Kumar, Taylor, Shi, Wang, et al. 2015). The ex vivo model system provides a critical framework for more translational in vivo pulp-capping experiments by validating the compatibility of the MDP scaffold in intact pulp tissue. This system can also be employed to test the effectiveness of the MDP scaffold as a delivery vehicle for regenerative bioactive materials into specific target tissues (Wickremasinghe et al. 2014).

Conclusion

This ex vivo organ culture model system has shown that the K(SL)₃RG(SL)₃KGRGDS MDP scaffold is compatible with the dental pulp and promotes differential responses depending on cell type. When the scaffold is delivered into the odontoblast space, the odontoblasts remain intact and synthetically active, possibly remodeling the injected scaffolds and preserving mineralizing activity at their margins. Furthermore, the MDP scaffold appears to act as a reservoir for a key dentin-specific matrix protein. The scaffold can alternatively be delivered to the pulp core without triggering mineralization or interfering with the native tissue architecture, and it appears to partially undergo degradation and remodeling.

Author Contributions

A.N. Moore, contributed to data analysis, acquisition and interpretation, drafted and critically revised the manuscript; S.C. Perez, contributed to data analysis and acquisition, drafted the manuscript; J.D. Hartgerink, contributed to design and data interpretation, critically revised the manuscript; R.N. D'Souza, contributed to data interpretation, critically revised the manuscript; J.S. Colombo, contributed to conception, design, data analysis, acquisition and interpretation,

drafted and critically revised the manuscript. All authors gave final approval and agree to be accountable for all aspects of the work.

References

Al-Hezaimi K, Salameh Z, Al-Fouzan K, Al Rejaie M, Tay FR. 2011. Histomorphometric and micro–computed tomography analysis of pulpal response to three different pulp capping materials. J Endod. 37(4):507–512.

Albuquerque MT, Valera MC, Nakashima M, Nör JE, Bottino MC. 2014. Tissue-engineering-based strategies for regenerative endodontics. J Dent Res. 93(12):1222–1231.

Aulisa L, Dong H, Hartgerink JD. 2009. Self-assembly of multidomain peptides: sequence variation allows control over cross-linking and viscoelasticity. Biomacromolecules. 10(9):2694–2698.

Bakota EL, Wang Y, Danesh FR, Hartgerink JD. 2011. Injectable multidomain peptide nanofiber hydrogel as a delivery agent for stem cell secretome. Biomacromolecules. 12(5):1651–1657.

Cavalcanti BN, Zeitlin BD, Nör JE. 2013. A hydrogel scaffold that maintains viability and supports differentiation of dental pulp stem cells. Dent Mater. 29(1):97–102.

Colombo JS, Balani D, Sloan AJ, Crean SJ, Okazaki J, Waddington RJ. 2011. Delayed osteoblast differentiation and altered inflammatory response around implants placed in incisor sockets of type 2 diabetic rats. Clin Oral Implants Res. 22(6):578–586.

Colombo JS, Howard-Jones RA, Young FI, Waddington RJ, Errington RJ, Sloan AJ. 2015. A 3D ex vivo mandible slice system for longitudinal culturing of transplanted dental pulp progenitor cells. Cytometry A. 87(10):921–928.

Colombo JS, Moore AN, Hartgerink JD, D'Souza RN. 2014. Scaffolds to control inflammation and facilitate dental pulp regeneration. J Endod. 40(4):S6–S12.

Cooper PR, Smith AJ. 2013. Molecular mediators of pulp inflammation and regeneration. Endod Top. 28(1):90–105.

D'Souza RN, Bronckers A, Happonen RP, Doga D, Farach-Carson M, Butler W. 1992. Developmental expression of a 53 KD dentin sialoprotein in rat tooth organs. J Histochem Cytochem. 40(3):359–366.

Dobie K, Smith G, Sloan A, Smith A. 2002. Effects of alginate hydrogels and TGF-β1 on human dental pulp repair in vitro. Connect Tiss Res. 43(2–3):387–390.

Farges JC, Keller JF, Carrouel F, Durand SH, Romeas A, Bleicher F, Lebecque S, Staquet, MJ. 2009. Odontoblasts in the dental pulp immune response. J Exp Zool B Mol Dev Evol. 312(5):425–436.

Furey A, Hjelmhaug J, Lobner D. 2010. Toxicity of Flow Line, Durafill VS, and Dycal to dental pulp cells: effects of growth factors. J Endod. 36(7):1149–1153.

Galler KM, Aulisa L, Regan KR, D'Souza RN, Hartgerink JD. 2010. Self-assembling multidomain peptide hydrogels: designed susceptibility to enzymatic cleavage allows enhanced cell migration and spreading. J Am Chem Soc. 132(9):3217–3223.

Galler KM, Hartgerink JD, Cavender AC, Schmalz G, D'Souza RN. 2012. A customized self-assembling peptide hydrogel for dental pulp tissue engineering. Tissue Eng Part A. 18(1–2):176–184.

Gebhardt M, Murray PE, Namerow KN, Kuttler S, Garcia-Godoy F. 2009. Cell survival within pulp and periodontal constructs. J Endod. 35(1):63–66.

Hilton TJ, Ferracane JL, Mancl L; Northwest Practice-based Research Collaborative in Evidence-based Dentistry. 2013. Comparison of CaOH with MTA for direct pulp capping: a PBRN randomized clinical trial. J Dent Res. 92(7):16S-22S.

Hincapié S, Fuks A, Mora I, Bautista G, Socarras F. 2015. Teaching and practical guidelines in pulp therapy in primary teeth in Colombia–South America. Int J Paediatr Dent. 25(2):87–92.

Hirschman WR, Wheater MA, Bringas JS, Hoen MM. 2012. Cytotoxicity comparison of three current direct pulp-capping agents with a new bioceramic root repair putty. J Endod. 38(3):385–388.

Kang MK, Colombo JS, D'Souza RN, Hartgerink JD. 2014. Sequence effects of self-assembling multidomain peptide hydrogels on encapsulated SHED cells. Biomacromolecules. 15(6):2004–2011.

Kobayashi M, Tsutsui TW, Kobayashi T, Ohno M, Higo Y, Inaba T, Tsutsui T. 2013. Sensitivity of human dental pulp cells to eighteen chemical agents used for endodontic treatments in dentistry. Odontology. 101(1):43–51.

Kumar VA, Taylor NL, Shi S, Wang BK, Jalan AA, Kang MK, Wickremasinghe NC, Hartgerink JD. 2015. Highly angiogenic peptide nanofibers. ACS Nano. 9(1):860–868.

Kumar VA, Taylor NL, Shi S, Wickremasinghe NC, D'Souza RN, Hartgerink JD. 2015. Self-assembling multidomain peptides tailor biological responses through biphasic release. Biomaterials. 52:71–78.

Mente J, Hufnagel S, Leo M, Michel A, Gehrig H, Panagidis D, Saure D, Pfefferle T. 2014. Treatment outcome of mineral trioxide aggregate or calcium hydroxide direct pulp capping: long-term results. J Endod. 40(11):1746–1751.

Mozayeni MA, Milani AS, Marvasti LA, Asgary S. 2012. Cytotoxicity of calcium enriched mixture cement compared with mineral trioxide aggregate and intermediate restorative material. Aust Endod J. 38(2):70–75.

Ng MH, Duski S, Tan KK, Yusof MR, Low KC, Rose IM, Mohamed Z, Bin Saim A, Idrus RB. 2014. Repair of segmental load-bearing bone defect by autologous mesenchymal stem cells and plasma-derived fibrin impregnated ceramic block results in early recovery of limb function. Biomed Res Int. 2014:345910.

Roberts JL, Maillard JY, Waddington RJ, Denyer SP, Lynch CD, Sloan AJ. 2013. Development of an ex vivo coculture system to model pulpal infection by *Streptococcus anginosus* group bacteria. J Endod. 39(1):49–56.

Ruan JL, Tulloch NL, Muskheli V, Genova EE, Mariner PD, Anseth KS, Murry CE. 2013. An improved cryosection method for polyethylene glycol hydrogels used in tissue engineering. Tissue Eng Part C Methods. 19(10):794–801.

Schmalz G. 2014. Pulp reactions to dental materials. In: Goldberg M, editor. The dental pulp: biology, pathology, and regenerative therapies. Berlin (Germany): Springer-Verlag Berlin Heidelberg. p. 169–183.

Sloan AJ, Taylor S, Smith EL, Roberts JL, Chen L, Wei XQ, Waddington, RJ. 2013. A novel ex vivo culture model for inflammatory bone destruction. J Dent Res. 92(8):728–734.

Smith EL, Locke M, Waddington RJ, Sloan AJ. 2010. An ex vivo rodent mandible culture model for bone repair. Tissue Eng Part C Methods. 16(6):1287–1296.

Song M, Kang M, Kim HC, Kim E. 2015. A randomized controlled study of the use of ProRoot mineral trioxide aggregate and Endocem as direct pulp capping materials. J Endod. 41(1):11–15.

Wickremasinghe NC, Kumar VA, Hartgerink JD. 2014. Two-step self-assembly of liposome-multidomain peptide nanofiber hydrogel for time-controlled release. Biomacromolecules. 15(10):3587–3595.

Xu D, Jiang L, Singh A, Dustin D, Yang M, Liu L, Lund R, Sellati TJ, Dong H. 2014. Designed supramolecular filamentous peptides: balance of nanostructure, cytotoxicity and antimicrobial activity. Chem Commun (Camb). 51(7):1289–1292.

Zmener O, Lalis RM, Pameijer CH, Chaves C, Kokubu G, Grana D. 2012. Reaction of rat subcutaneous connective tissue to a mineral trioxide aggregate–based and a zinc oxide and eugenol sealer. J Endod. 38(9):1233–1238.